Solution Conformation of a Peptide Corresponding to the Principal Neutralizing Determinant of HIV-1_{IIIB}: A Two-Dimensional NMR Study†

Anat Zvi, Reuben Hiller,‡ and Jacob Anglister*

Department of Structural Biology, The Weizmann Institute of Science, Rehovot 76100, Israel

Received February 3, 1992; Revised Manuscript Received April 28, 1992

ABSTRACT: The 24 amino acid peptide RP135 corresponds in its amino acid sequence to the principal neutralizing determinant (PND) of the IIIB isolate of HIV-1. Although the sequence of the PND is highly variable, its central part, containing the sequence GPGR, is conserved in most HIV isolates. Using 2D NMR and CD spectroscopy, we have studied the conformation of RP135 and of two shorter versions: one (P547) that includes the GPGR sequence with the N-terminal part of the peptide and the other (P344) that includes GPGR and the C-terminal segment of RP135. In water, the C-terminal part of RP135 was found to exist in several transient turnlike conformations ("nascent helix"). A helical conformation was found to be stabilized by the addition of TFE. A transient turn was observed also in the GPGR sequence, both in water and in aqueous TFE solutions. While no nascent helix conformations could be observed in the N-terminal part of RP135 in water, a helical conformation was partially stabilized by the addition of TFE. The conformations of the two shorter versions of the peptide were similar to those of the corresponding parts of RP135, except that the transient turn in GPGR could not be detected in P547 dissolved in water. The turn in GPGR was previously predicted by Larosa et al. (1990) and was observed by Chandrasekhar et al. (1991) in the PND peptide of HIV-1_{MN} (RP142), which shares only 56% identity with RP135. However, nascent helix conformations were not observed in aqueous solutions of RP142. It is possible that the mutations, deletions, and insertions in the PND peptides modulate their tendency to form nascent helix conformations in water, without affecting the formation of a turn in the conserved GPGR sequence.

The envelope glycoprotein (gp120)[1] of the human immunodeficiency virus type 1 (HIV-1) plays a major role in the infection of healthy T-cells by the virus. Infection is made possible by the binding of gp120, found on the surface of the virus and virus-infected cells, to CD4, a protein present on the membranes of helper T-cells. The envelope glycoprotein of HIV-1 is the target for neutralizing antibodies and therefore has the potential for use as a subunit vaccine. Unfortunately, for vaccine development, the amino acid sequence of this protein varies among different isolates of the virus, and consequently the antibody neutralizing activity is strain-specific. Another obstacle is the fact that gp120 contains determinants that elicit the production of antibodies which enhance infection of healthy cells by the virus (Robinson et al., 1989, 1990; Takeda et al., 1988).

Most of the HIV-1 neutralizing activity in infected individuals or immunized animals is against a determinant located within the third hypervariable region of gp120, between two cysteine residues (Cys-303 and Cys-338) forming a disulfide bridge (Rusche et al., 1988; Palker et al., 1988; Goudsmit et al., 1988). This determinant was termed the "principal neutralizing determinant" (PND) and was mapped to a 24 amino acid long sequence denoted RP135. The peptide RP135 or its shorter versions, when used as immunogens, were found to elicit virus neutralizing antibodies, thus demonstrating their potential use in a peptide-based vaccine (Palker et al., 1988). Moreover, RP135 contains an epitope for the T-cell receptors of CD4+ helper T-cells and the only gp120 epitope for the receptors of CD8+ cytotoxic T-cells (Takahashi et al., 1988, 1990). The mechanism of virus neutralization by antibodies recognizing the PND is not yet clear. Although these antibodies do not prevent binding of the virus to their target cells, they do inhibit fusion of the virus and virus-infected cells with healthy T-cells.

To define the epitopes within the PND that are responsible for inducing HIV-1 neutralizing antibodies, the fine specificity of several murine monoclonal antibodies against gp120 of HIV-1_{IIIB} was investigated. Skinner et al. (1988) postulated that the neutralizing antibody 0.5β (Matsushita et al., 1988) recognizes a sequence that includes a hypothetical tip (GPGR) of the loop and a sequence on its C-terminal side (RGPGRAFVTIGKIG) while another antibody, 9284, recognizes a sequence in the N-terminal side of GPGR (NNTRKSIRIQRG). Liou et al. (1989) found that the BAT123 antibody recognizes the sequence RIQRGPGRAFVTIGK. Similarly, it was found that human monoclonal antibodies that neutralize HIV-1_{MN} recognize different epitopes within the PND (Gorny et al., 1991; Scott et al., 1990). In a complementary approach to define smaller neutralizing epitopes within the PND, pep-

† We gratefully acknowledge financial support from the Minerva Foundation, Munich, Germany, the Crown Endowment Fund for Immunological Research at the Weizmann Institute of Science, and the Helen and Milton Kimmelman Center for Biomolecular Structure.

* To whom correspondence should be addressed. J.A. is the incumbent of the Graham and Rhona Beck Career Development Chair.

‡ Levi Eshkol Postdoctoral Fellow. Present address: Department of Biochemistry and Biophysics, 338 Anatomy Chemistry Building, University of Pennsylvania, Philadelphia, PA 19104-6059

[1] Abbreviations: CD, circular dichroism; CD4, protein found on the membrane of helper T-cells; DQF-COSY, double-quantum-filtered 2D *J*-correlated spectroscopy; gp120, envelope glycoprotein of HIV-1_{IIIB}; HOHAHA, homonuclear Hartman-Hahn 2D experiment; HIV, human immunodeficiency virus; HPLC, high-performance liquid chromatography; NMR, nuclear magnetic resonance; NOE, nuclear Overhauser effect; NOESY, 2D NOE spectroscopy; PND, principal neutralizing determinant; P344, peptide containing the C-terminal part of RP135; P547, peptide containing the N-terminal part of RP135; RP135, PND of gp120; TFE, trifluoroethanol; TPPI, time-proportional phase incrementation method; 2D, two-dimensional.

0006-2960/92/0431-6972$03.00/0

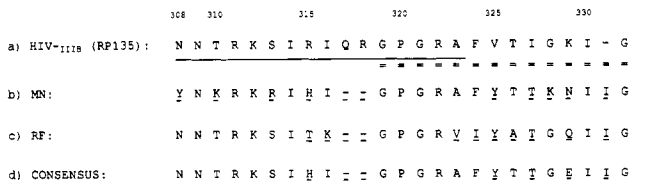

FIGURE 1: Amino acid sequence of the PNDs of common HIV isolates aligned with the consensus sequence; the sequences corresponding to P547 and P344 are indicated by a dashed line and a double-dashed line, respectively; the underlined residues represent mutations relative to RP135.

tide immunogens of different lengths and sequences have been used to induce virus neutralizing antibodies (Javaherian et al., 1990; Wang et al., 1991; Holley et al., 1991).

Larosa et al. (1990) analyzed the amino acid sequences of the PND of 245 different isolates to check the feasibility of using PND peptides to induce antibodies that neutralize a broad spectrum of viral strains. At every position of the PND sequence, one amino acid was found to occur at high frequency. A consensus sequence that has the most common amino acid for each position in the sequence was derived. PND peptides comprising the consensus sequence have been postulated as likely to induce antibodies that neutralize a majority of HIV-1 isolates. The most conserved pattern within the PND is the GPG tripeptide (residues 319–321), present in 97% of the isolates. Six amino acid peptides (IGPGRA and GPGRAF) that include the tip are common to more than 60% of HIV-1 isolates. Up to 71% of randomly selected HIV-1-positive human sera reacted with three different peptides, comprising the amino acid sequences of the SC, MN, and WMJ2 isolates. Multivalent synthetic peptides containing PND sequences from three different isolates (IIIB, RF, and MN) were shown to induce neutralizing antibodies to each of these isolates (Palker et al., 1990). These results demonstrate that selecting an appropriate combination of peptides from different variants, together with choosing the most conserved regions of the PND, may produce candidate vaccines that induce antibodies capable of neutralizing the majority of HIV-1 strains.

A better understanding of the molecular basis for the cross-reactivity of antipeptide antibodies with native proteins can be obtained by studies of the conformations of free immunogenic peptides and comparison with those of the antibody-bound peptides and of the corresponding parts of the proteins. The solution conformations of three immunogenic peptides derived from the principal neutralizing determinant (PND) of the MN isolate were recently studied (Chandrasekhar et al., 1991). It has been postulated that, in aqueous solutions of the PND of the MN isolate and the peptide containing the whole loop, there is a significant population of conformations containing a β-turn in the highly conserved sequence GPGR. The NMR spectra exhibited conformational averaging for the other segments of the two HIV-1_{MN} peptides.

We present here a 2D NMR and CD study of the conformation of RP135 (NNTRKSIRIQRGPGRAFVTIGKIG) in water and in aqueous solutions containing TFE. RP135 is the PND peptide of the HIV-1_{IIIB} isolate (BRU) (Ratner et al., 1985; Wain-Hobson et al., 1985) which was the first HIV-1 variant to be isolated and has been the most studied. RP135 differs considerably in its amino acid sequence from the RP142 peptide studied by Chandrasekhar et al. (1991). Alignment of the PND of HIV-1_{IIIB} with the consensus sequence and the sequences of the PND of the most common isolates of HIV-1 is shown in Figure 1. We also studied the conformation of two shorter versions of RP135: P547, which includes the conserved tip and the sequence on the N-terminal side (NNTRKSIRIQRGPGRA), and P344, which contains the tip and the sequence on the C-terminal side, with the addition of the GKK sequence to increase its solubility in water (GPGRAFVTIGKIGGKK). For the design of a minimal cocktail of peptides to be used in a synthetic vaccine, it is important to study the relationship between sequence diversity and the conformations of the PND peptides. The two peptides, P547 and P344, were studied to find out whether shorter peptides, that are often used as immunogens, have conformations similar to those of the whole PND peptide.

MATERIALS AND METHODS

Peptides were synthesized using an Applied Biosystem 430A automated peptide synthesizer. Crude peptides were partially purified by gel filtration chromatography on a G-25 column equilibrated with 0.5% acetic acid in water. Better than 98% purity was obtained by further purification using high-performance liquid chromatography (HPLC), with acetonitrile/water mixtures containing trifluoroacetic acid to elute the peptides. The amino acid composition of the purified peptides was verified by amino acid analysis. Peptide concentrations were 2–5 mM, in 10 mM phosphate- or acetate-buffered 90% H_2O/10% D_2O solutions containing 0.05% sodium azide, at pH 4.8 or 6. Aqueous TFE solutions contained 30% (v/v) or 60% TFE and no D_2O.

NMR Measurements. All NMR measurements were carried out at 500 MHz, on a Bruker AM-500 spectrometer, in the phase-sensitive mode, using the time-proportional phase incrementation method (TPPI) (Marion & Wüthrich, 1983). HOHAHA (Bax et al., 1985) and NOESY (Macura et al., 1981) experiments were carried out by regular procedures. In the HOHAHA experiments, the carrier was set on the water resonance, and the HDO signal was presaturated before the first 90° pulse. In the NOESY experiments, the HDO signal was suppressed by a selective excitation using the "jump and return" pulse sequence (Plateau & Guéron, 1982). NOESY spectra were measured using 100-, 200-, and 400-ms mixing times. In these experiments, 2048 data points in F2 and at least 512 t1 increments were collected in a spectral width of 10 ppm in both dimensions. In the HOHAHA experiments, 8196 data points in F2 were collected to increase the spectral resolution for determining the $^3J_{NH}$ coupling constants. The relaxation delays were 1.2 s in the HOHAHA experiments and 3 s in the NOESY experiments. A 10% random variation in the mixing time was used in the NOESY experiments to eliminate cross-peaks due to coherent transfer. Typically, 64–96 transients were collected for each increment of t1 in the NOESY experiments, and 16–72 scans were acquired in the HOHAHA experiments.

Most of the measurements were carried out at 4 °C (except for P344 in TFE, when the experiments were carried out also at −4 °C, to increase the population of the most stable conformation and the intensity of the NOE). The broadening of the amide proton resonances of the peptide in TFE solutions prevented the determination of the J coupling at 4 °C. To measure the coupling constants, additional HOHAHA measurements were carried out at 10 and 15 °C. The problems encountered in DQF-COSY when the line width approaches the value of the coupling constants are alleviated in the HOHAHA measurements (Neuhaus, 1985).

Data processing was carried out on a Bruker X32 workstation. The data were zero-filled in F1 and multiplied by a sine window function shifted by 22.5° (for the NOESY experiments) or 45° (for the HOHAHA experiments) before

Fourier-transformation. The spectra were calibrated with tetramethylsilane and were base-line-corrected by a Bruker program that divided the spectrum into two parts around the water signal in the F2 dimension, allowing definition of a window around the water which was not base-line-corrected. A polynomial base-line correction was then applied to each part separately. The spectra were not symmetrized.

Circular Dichroism Spectroscopy. CD spectra were recorded on a JASCO-500C spectrometer, at ambient temperature, in a cell of 0.01-cm path length. CD samples contained 0.3–0.5 mg/mL peptide in aqueous solutions buffered with 10 mM phosphate at pH 4.8 and containing various concentrations of TFE. The spectra are presented as a plot of the mean molar ellipticity per residue ($[\theta]$, in degrees centimeter squared per decimole). Analysis of the CD data was carried out according to the method developed by Chen et al. (1974) which uses spectra of proteins that have a known secondary structure as reference.

RESULTS

Resonance Assignments of the Peptides. The ^{1}H resonances in the NMR spectra of the peptides (Table I) were assigned by the sequential assignment methodology developed by Wüthrich and his co-workers (Wüthrich, 1986) using NOESY and HOHAHA spectra measured consecutively and under the same conditions. In the first stage, the complete spin systems of the individual amino acid residues were identified using HOHAHA spectra measured in H_2O. In the next stage, the backbone sequential connectivities were established by following the fingerprint region of the HOHAHA and NOESY spectra.

Secondary Structure of RP135 and Its Derivatives in H_2O. For measurements in water, we used the peptide RP135-GKK, which comprises RP135 with the sequence Gly-Lys-Lys added to its carboxy terminus to increase its solubility. The NOESY spectrum of RP135-GKK measured at pH 6.0 with 400-ms mixing time is shown in Figure 2. Additional measurements were carried out at pH 4.8, using mixing times of 100 and 400 ms. In all three measurements, a stretch of $d_{NN}(i,i+1)$ connectivities was observed from Gly-14 to Gly-25, with the exceptions of Ala-16 interaction with Phe-17 and Thr-19 interaction with Ile-20, which were not observed due to degeneracy in the chemical shift of their amide proton resonances. In the N-terminal part of the peptide, we observed amide proton interactions between Ile-7 and Arg-8 and between Ile-9 and Gln-10. The observation of these interactions between adjacent residues indicates that in water there is a significant population of conformers with dihedral angles in the α_R region of the (ϕ,ψ) space. At the same time, we observed relatively strong $d_{\alpha N}(i,i+1)$ connectivities along the whole peptide, indicative of an extended chain or β-strands. Further examination of the NOESY spectra revealed a number of $d_{\alpha N}(i,i+2)$ NOE's in the C-terminal part of the peptide. These interactions are typical of β-turns, indicating that β-turns are formed in a significant population of the peptide molecules. Also, a very weak interaction appeared between the δ-proton of Pro-13 and the amide proton of Gly-14. This interaction may indicate a small population in a type I β-turn formed by GPGR. No medium- or long-range interactions within the peptide which would indicate the presence of a helix or a β-sheet were detected. The $^3J_{NH}$ coupling constants measured at 4 °C were in the range of 6.1–7.3 Hz for all the amide protons in the peptide backbone, indicating an equilibrium between several conformers.

The temperature dependence of the chemical shift of the amide protons was studied by measuring HOHAHA spectra

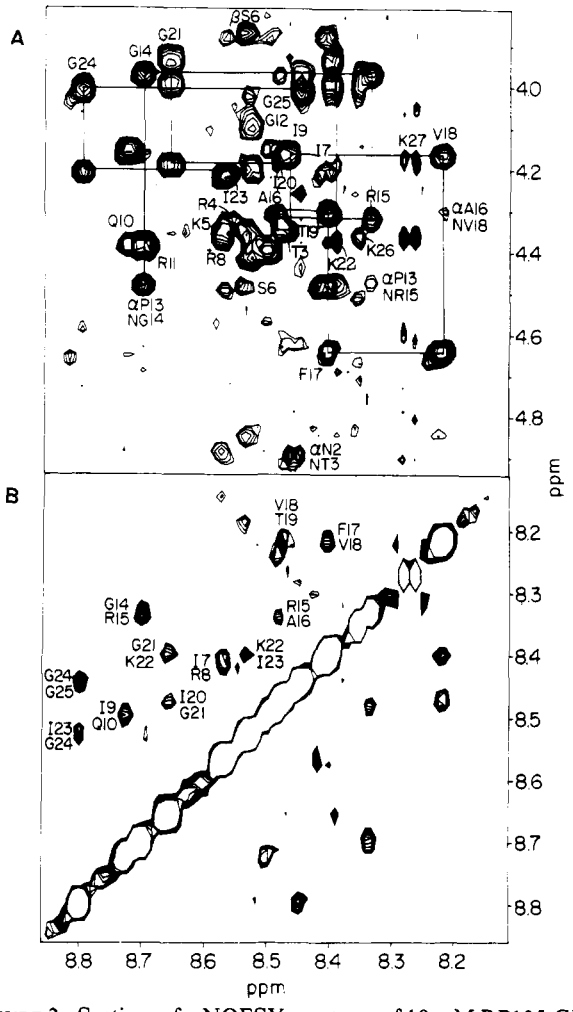

FIGURE 2: Sections of a NOESY spectrum of 10 mM RP135-GKK in 90% H_2O/10% D_2O at pH 6.0, measured at 4 °C using a mixing time of 400 ms. (A) NH–C_αH region; several sequential pathways are drawn; (B) NH–NH region.

with lower resolution in F2 (2048 data points) at 4 different temperatures: 4, 14, 24, and 34 °C, at pH 4.8. Two-dimensional spectra were measured to alleviate problems of resonance overlap. Temperature coefficients ($-\Delta\delta/\Delta T \times 10^3$ ppm/K) were determined for 17 out of 27 peptide residues. The measured temperature coefficients were found to be between 7.3×10^{-3} and 10×10^{-3} ppm/K. The lowest values were for Arg-15, Val-18, Gly-25, and Lys-26: 8.0×10^{-3}, 7.7×10^{-3}, 7.3×10^{-3}, and 8.0×10^{-3} ppm/K, respectively. The amide protons of the first three residues were found to be involved with the detected $d_{\alpha N}(i,i+2)$ interactions which characterize the reverse turn. An overlap with the $d_{\alpha N}(i,i+1)$ interaction between Gly-25 and Lys-26 prevented detection of the $d_{\alpha N}(i,i+2)$ interaction between Gly-24 and Lys-26. The average temperature coefficient for the other residues of RP135-GKK was 9.2×10^{-3} ppm/K.

A section of the NOESY spectrum of P344 (GP-GRAFVTIGKIGGKK), which includes the postulated tip and the sequence on its C-terminal side, is shown in Figure 3A. In this spectrum, which was measured in H_2O, we observed strong $d_{\alpha N}(i,i+1)$ and only weak $d_{NN}(i,i+1)$ NOE's. In addition, very weak $d_{\alpha N}(i,i+2)$ connectivities between Pro-13 and Gly-15, Ala-16 and Val-18, and Gly-21 and Ile-23 were detected. No other medium- or long-rang NOE's were observed. These results indicate the presence of a conformational population in the β region of the (ϕ,ψ) space, in equilibrium with a small, but not negligible, population of

Table I: ^{1}H Resonance Assignments

residue	chemical shifts (ppm)[a] NH	αH	βH	others
Asn-1				
Asn-2	8.99	4.86	2.90, 2.82	
Thr-3	8.46	4.35	4.14	γCH$_3$, 1.22
Arg-4	8.53	4.34	1.89	γCH$_2$, 1.64; δCH$_2$, 3.19
Lys-5	8.57	4.34	1.85	γCH$_2$, 1.45; δCH$_2$, 1.75, 1.69; εCH$_2$, 3.02
Ser-6	8.54	4.48	3.85	
Ile-7	8.41	4.22	1.88	γCH$_2$, 1.47; γCH$_3$, 0.91; δCH$_3$, 0.86
Arg-8	8.57	4.35	1.89	γCH$_2$, 1.69; δCH$_2$, 3.18
Ile-9	8.47	4.19	1.81	γCH$_2$, 1.53; γCH$_3$, 0.94; δCH$_3$, 0.87
Gln-10	8.72	4.38	2.08, 1.98	γCH$_2$, 2.36
Arg-11	8.69	4.42	1.88, 1.78	γCH$_2$, 1.66; δCH$_2$, 3.19
Gly-12	8.52	4.09		
Pro-13		4.48	2.29, 2.03	γCH$_2$, 2.03; δCH$_2$, 3.88, 3.68
Gly-14	8.70	3.97		
Arg-15	8.33	4.32	1.81, 1.72	γCH$_2$, 1.59; δCH$_2$, 3.18; NH, 7.27
Ala-16	8.48	4.29	1.33	
Phe-17	8.40	4.64	3.10, 3.04	2,6H, 7.24; 4H, 7.32; 3,5H, 7.37
Val-18	8.21	4.16	1.99	γCH$_3$, 0.90
Thr-19	8.45	4.32	4.25	γCH$_3$, 1.24
Ile-20	8.49	4.16	1.84	γCH$_2$, 1.51; γCH$_3$, 0.89; δCH$_3$, 0.89
Gly-21	8.68	3.96		
Lys-22	8.39	4.38	1.83	γCH$_2$, 1.41; δCH$_2$, 1.75, 1.69; εCH$_2$, 3.02
Ile-23	8.52	4.21	1.89	γCH$_2$, 1.54; γCH$_3$, 0.94; δCH$_3$, 0.88
Gly-24	8.80	4.01		
Gly-25	8.44	4.00		
Lys-26	8.35	4.37	1.87	γCH$_2$, 1.45; δCH$_2$, 1.77, 1.69; εCH$_2$, 3.01
Lys-27	8.26	4.17	1.83	γCH$_2$, 1.42; δCH$_2$, 1.73, 1.69; εCH$_2$, 3.01

[a] Chemical shifts of RP135-GKK in H_2O, pH 6, T = 4 °C.

conformers in the α region. The $d_{\alpha N}(i,i+2)$ indicates the formation of transient reverse turns. With regard to the P547 peptide (NNTRKSIRIQRGPGRA-amide), only strong $d_{\alpha N}(i,i+1)$ connectivities were detected in its NOESY spectrum measured in H_2O; the $^3J_{NH}$ values were between 6.1 and 7.3 Hz, indicating averaging between different conformations. The $d_{\alpha N}(i,i+2)$ interaction between Pro-13 and Gly-15 could not be detected because of overlap with the strong $d_{\alpha N}(i,i+1)$ interaction between Ser-6 and Ile-7.

Circular Dichroism Measurements of the Peptides. The NMR spectra of RP135-GKK and P344 show short-range interactions indicative of a population in a folded conformation (reverse turn or helix). However, medium- and long-range interactions characteristic of a helical conformation were not detected. To obtain further information on conformations of the peptides in aqueous solutions, we measured their CD spectra in the near-UV and at room temperature. They were found to resemble typical spectra of an extended conformation, indicating that only a negligible population of the peptide molecules is in a helical conformation (at most 10%). To determine whether a helical conformation can be stabilized, we prepared peptide solutions containing 20–60% (v/v) trifluoroethanol (TFE), which is known to be a helix stabilizer (Clore et al., 1986; Marion et al., 1988; Lehrman et al., 1990). Indeed, addition of TFE to aqueous solutions of the peptides resulted in the appearance of maximum ellipticity at 190 nm and a minimum at 208 nm, which are typical of a helical conformation. Increasing concentrations of TFE caused an increase in the absolute values of the ellipticity at the above wavelengths. At 30% TFE, the peptides RP135, RP135-GKK, and P344 have already almost reached their asymptotic helical content, which was found to be 35, 40, and 50%, respectively. P547 showed negligible helical conformation in aqueous solutions containing 20 and 30% TFE, and only 25% helical conformation in 60% TFE solutions. The CD spectra of RP135-GKK, RP135, P344, and P547 in aqueous solutions containing increasing concentrations of TFE are shown in Figure 4. Comparison of the CD spectra of RP135-GKK and RP135 shows that addition of the GKK sequence did not have any detectable influence on the peptide conformation.

NMR Studies of the PND Peptides in Aqueous TFE Solutions. The NOESY spectrum of RP135 in 30% TFE/70% H_2O was measured at 4 °C and is shown in Figure 5. In comparison to the NOESY spectrum of RP135-GKK in water (Figure 2), in the spectrum measured in TFE/H_2O we observed stronger $d_{NN}(i,i+1)$ connectivities as well as a decrease in the intensity of the corresponding $d_{\alpha N}(i,i+1)$ connectivities. Some additional $d_{\alpha N}(i,i+2)$ NOE's appeared, two of them in the N-terminal part of the peptide. Medium-range interactions, $d_{\alpha N}(i,i+3)$ and $d_{\alpha\beta}(i,i+3)$, which are typical of a helical conformation, were not observed. The $^3J_{NH}$ coupling constants of RP135 were determined from its HOHAHA spectrum measured at 15 °C instead of at 4 °C to obtain sharper resonances for the amide protons. The values for the $^3J_{NH}$ coupling constants revealed differing trends between the two parts of the peptide: amino acids residing in the N-terminal segment had coupling constants of 6.1 Hz (with the exception of Ser-6 and Gln-10 for which the coupling constant was 4.9 Hz); in the C-terminal segment, most of the $^3J_{NH}$ values were found to be 4.9 Hz, with the exception of the amide protons of Lys-22 and Ile-23 for which a 6.1-Hz coupling constant was measured.

In the NOESY spectrum of P344 in 30% TFE/70% H_2O, we observed a considerable increase in the intensity of the $d_{NN}(i,i+1)$ cross-peaks (Figure 3B). Only one medium-range interaction, $d_{\alpha N}(i,i+3)$, was observed, between Lys-22 and Gly-25. The $^3J_{NH}$ coupling constants of the peptide amide protons determined from the HOHAHA spectrum of the peptide measured at 10 °C were in the range 3.7–4.9 Hz (with the exception of Lys-27).

The $^3J_{NH}$ coupling constants of the amide protons of P547 in 30% TFE/70% H_2O were determined from its high-resolution HOHAHA spectrum measured at 10 °C. Coupling constants less than 5 Hz were measured for Thr-3, Arg-4, Lys-5, and Ser-6 while for residues 7–16 the coupling constants were in the range 6.1–7.3 Hz. The NOESY spectrum of P547 containing 30% TFE shows $d_{NN}(i,i+1)$ connectivities, as well as weak $d_{\alpha N}(i,i+2)$ between Lys-5 and Ile-7, Gly-12 and Gly-14, and Gly-14 and Ala-16. The NOESY spectrum of P547 in 60% TFE/40% H_2O shows a stretch of $d_{NN}(i,i+1)$ and $d_{\alpha N}(i,i+2)$ NOE's along the whole peptide. We also observed $d_{NN}(i,i+2)$ connectivities and medium-range $d_{\alpha N}(i,i+3)$ connectivities between Asn-2 and Lys-5 and between Lys-5 and Arg-8 (Figure 6). None of these interactions were observed in aqueous solution of the peptide without TFE. Schematic diagrams summarizing the various connectivities observed in the NOESY spectra in water and in aqueous TFE solutions are shown in Figure 7.

DISCUSSION

Our NMR data indicate that RP135 in water is found in fast equilibrium between different conformations. This conclusion is supported by the observation of $^3J_{NH}$ coupling constants in the range of 6–7 Hz and strong $d_{\alpha N}(i,i+1)$, together with d_{NN} sequential NOE's. The absence of inter-

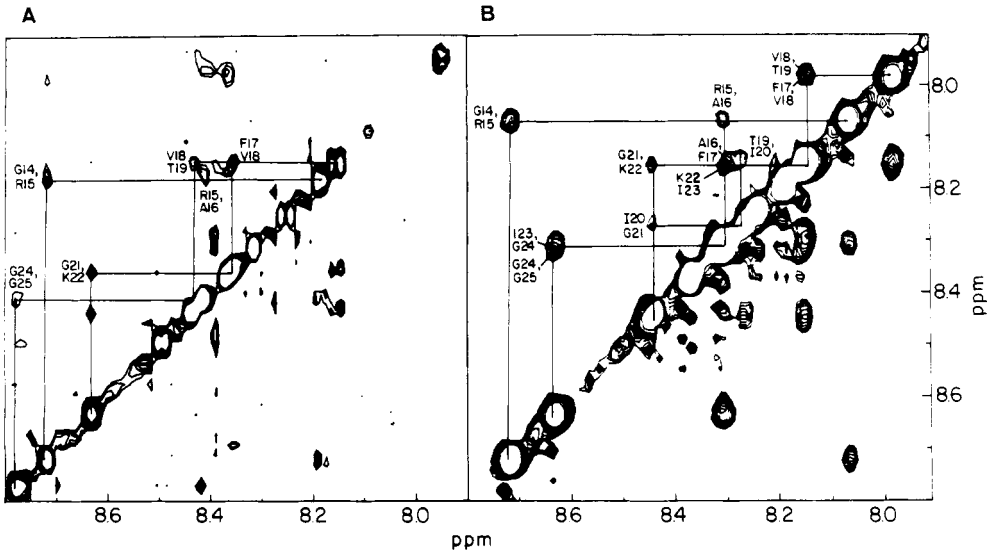

FIGURE 3: Sections of NOESY spectra of 10 mM P344 at pH 4.8 using a 200-ms mixing time. (A) In 90% H_2O/10% D_2O, measured at 4 °C; (B) in 30% TFE/70% H_2O, measured at −4 °C.

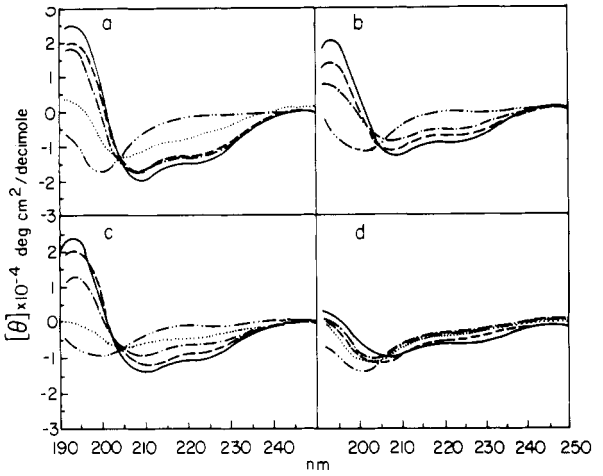

FIGURE 4: CD spectra of (a) RP135-GKK, (b) RP135, (c) P344, and (d) P547, at pH 4.8, measured at ambient temperature in H_2O (– •• –) and in solutions containing varying amounts of TFE: 20% (•••); 30% (– • –); 40% (– –); 60% (—); [θ] is the mean molar ellipticity per mole of residue.

strand $d_{\alpha\alpha}(i,j)$ and $d_{\alpha N}(i,j)$ rules out the possibility that any significant population exists in a β-sheet structure. The strong $d_{\alpha N}$ interactions are therefore indicative of a considerable population in extended conformations. The CD spectrum and the lack of medium-range interactions [$d_{\alpha\beta}(i,i+3)$, $d_{\alpha N}(i,i+3)$, and $d_{\alpha N}(i,i+4)$] in the NOESY spectrum of RP135-GKK indicate that in H_2O there is no significant population in a stable helical conformation. However, the presence of three weak $d_{\alpha N}(i,i+2)$ connectivities, the slightly lowered temperature coefficients for the chemical shifts of the amide protons involved in these interactions, and the presence of multiple d_{NN} sequential NOE's indicate that at least three transient turns are formed in the C-terminal part of the peptide in aqueous solution.

Addition of 30% TFE was found to stabilize a helical conformation in RP135, as observed by the appearance of a CD spectrum typical of a helical conformation, by reduced $^3J_{NH}$ coupling constants between 4.9 and 6.1 Hz, and by a diminution in the magnitude of the $d_{\alpha N}(i,i+1)$ versus the corresponding $d_{NN}(i,i+1)$ connectivities. Nevertheless, despite all these indications of the presence of a significant population in a helical conformation, no $d_{\alpha N}(i,i+3)$ and $d_{\alpha\beta}(i,i+3)$ medium-range interactions typical of a helical conformation

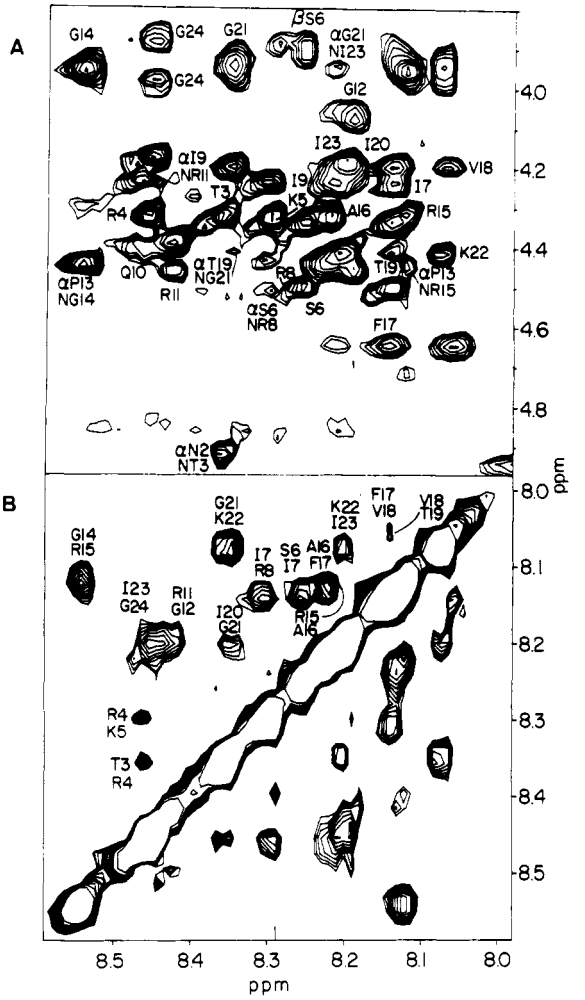

FIGURE 5: Sections of a NOESY spectrum of 5 mM RP135 in 30% aqueous TFE (v/v), containing 10 mM sodium acetate buffer, at pH 4.8, measured at 10 °C using a 200-ms mixing time. (A) NH–C_αH region; (B) NH–NH region.

were observed in TFE/H_2O solutions of RP135. The first type of interaction may have been masked by overlap with the crowded and much stronger $d_{\alpha N}$ and $d_{\alpha N}(i,i+1)$ interactions, while the second was not observed probably due to the already weak cross section for magnetization transfer for short peptides and a further reduction in the intensity because of the

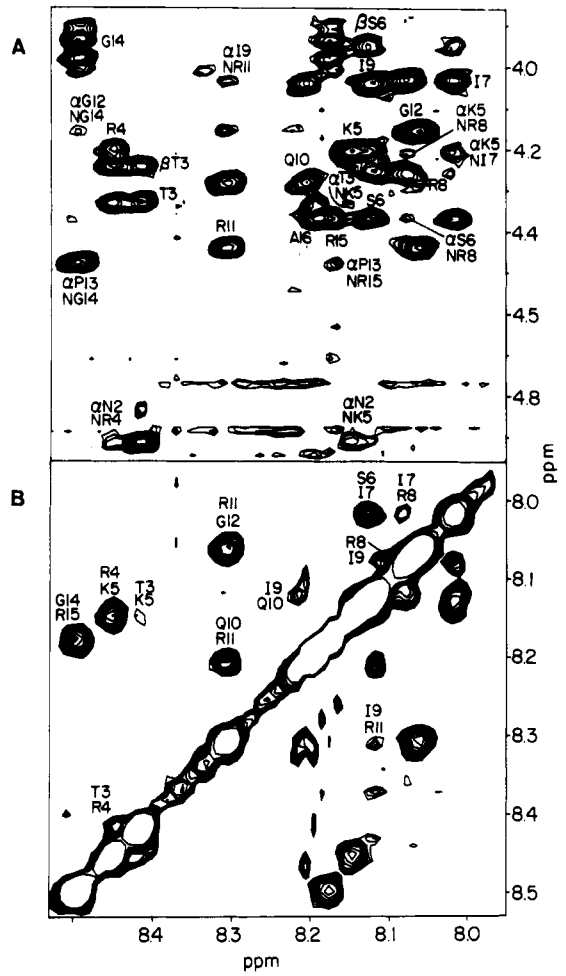

FIGURE 6: Portions of a NOESY spectrum of 5 mM P547 in 60% aqueous TFE containing 10 mM acetate buffer at pH 4.8, measured at 4 °C. A mixing time of 400 ms was used. (A) NH–C_αH region; (B) NH–NH region.

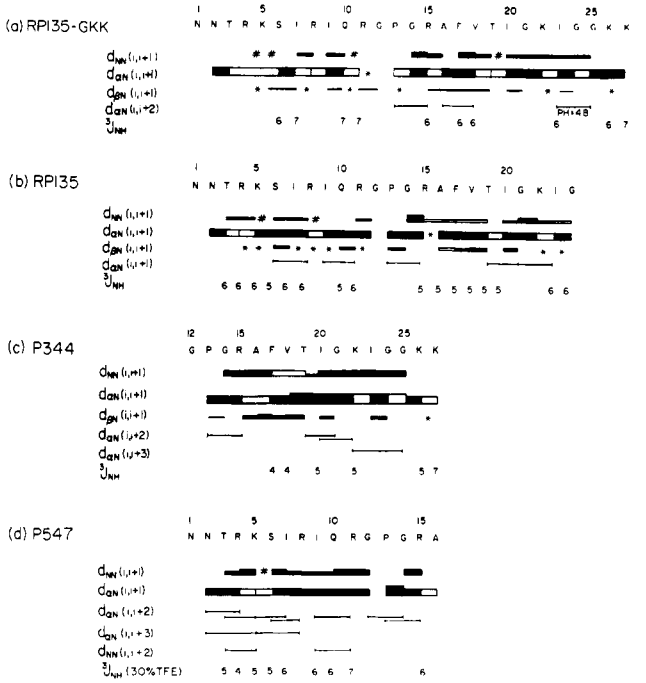

FIGURE 7: Schematic diagrams, summarizing the NOE connectivities and $^3J_{NH}$ coupling constants observed for the peptides: (a) RP135-GKK in 90% H_2O/10% D_2O; (b) RP135 in 30% aqueous TFE; (c) P344 in 30% aqueous TFE; (d) P547 in 60% aqueous TFE (v/v). An open square indicates that the intensity could not be determined due to overlap of two or more cross-peaks; an asterisk indicates overlap with another cross-peak; (#) indicates that the protons are degenerated.

increased flexibility of the side chains. The observation of strong $d_{\alpha N}(i,i+1)$ connectivities and several $d_{\alpha N}(i,i+2)$ connectivities indicates that the helical conformation is not the only conformation in TFE solutions and that a significant number of the molecules populate reverse turn and unfolded conformations, a conclusion that is supported by the helical content of the peptide determined from its CD spectrum. It is possible that the helical structure that is stabilized by TFE is a 3_{10}-helix rather than an α-helix, since the former is characterized by much weaker $d_{\alpha\beta}(i,i+3)$ interactions and stronger $d_{\alpha N}(i,i+2)$ interactions (Wüthrich et al., 1984; Wagner et al., 1986).

A similar situation was observed by Dyson et al. (1988) in their investigation of the solution conformation of an immunogenic peptide fragment of myohemerythrin. According to the X-ray structure, the corresponding region in the native protein forms a helix. These investigators explained the coexistence of $d_{\alpha N}(i,i+1)$, $d_{NN}(i,i+1)$, and $d_{\alpha N}(i,i+2)$ cross-peaks in the C-terminal part of the peptide in the NOESY spectrum of the peptide in H_2O, and the lack of the typical characteristics of helix in the CD spectrum, as due to the fact that the peptide consists of a set of turnlike structures distributed along the C-terminal part of the myohemerythrin peptide, rapidly interconverting through unfolded states. The term "nascent helix" was used to describe these conformations (Dyson et al., 1988). Addition of TFE stabilized a helical conformation only in the C-terminal segment of the myohemerythrin peptide without the appearance of sequential d_{NN} interactions in the N-terminal portion of the peptide. Thus, TFE stabilizes a helical conformation in a nascent helix, without causing the formation of a helix in peptide regions that in water did not have any significant population of conformers with dihedral angles in the αR region of the (ϕ,ψ) space.

The intensities of the NOE's are even weaker for the two shorter peptides, P344 and P547, because of their shorter correlation time. Nevertheless, we observed weak connectivities between the amide protons of adjacent amino acids and additional weak $d_{\alpha N}(i,i+2)$ connectivities in aqueous solution of the C-terminal containing peptide P344. These connectivities indicate that P344, like the corresponding part of RP135, has a tendency to exist in a nascent helix conformation. Under the same conditions, the N-terminal-containing peptide P547 does not show any detectable population in nascent helix conformations.

As with RP135, addition of TFE to P344 and P547 stabilizes a helical conformation, as affirmed by their CD and NMR spectra. The smaller number of cross-peaks in the spectral region showing $d_{\alpha N}$ and $d_{\alpha N}(i,i+1)$ interactions enabled us to detect a few $d_{\alpha N}(i,i+3)$ interactions that characterize a helical conformation and were not detected in the NOESY spectrum of RP135. The NOESY spectrum of P547 reveals a significant population in a helical conformation in a solution containing as little as 30% TFE. The helical conformation is characterized by strong sequential d_{NN} NOE's and weak medium-range NOE's, $d_{\alpha N}(i,i+3)$ and $d_{NN}(i,i+2)$. The $^3J_{NH}$ coupling constants of the amide protons of P547 indicate a helical conformation in the segment containing residues Asn-1 to Ser-6 and a conformational averaging in the remainder of the peptide. According to its CD spectrum, the tendency of P547 to form a helix is weaker than that anticipated from its NOESY spectrum. There may be two reasons for this discrepancy: (a) distortions within the helix coil, which result in a decrease

in the CD helix signal at 222 nm; and (b) the presence of a β-turn in the peptide, with a characteristic positive band at 224 nm, which partially cancels the negative helix peak at 222 nm (Bradley et al., 1990). The CD and NMR data indicate that in 30% TFE/70% H_2O solutions of the three peptides, there is still a significant fraction of the molecules in nascent helix conformations, as indicated by the observation of strong $d_{\alpha N}(i,i+1)$ connectivities and several weak $d_{\alpha N}(i,i+2)$ connectivities. The peptide P547 populates a helical conformation to a considerably lesser extent relative to P344.

The NOESY spectra of RP135 and P344 in water indicate that a significant population of the molecules exists in a conformation in which a turn is formed in the segment GPGR. However, under the same conditions, transient turns are formed in other parts of the peptide as well. Comparison of the intensities of the d_{NN} and $d_{\alpha N}(i,i+2)$ connectivities in the NOESY spectrum of RP135-GKK in H_2O shows that the d_{NN} interaction between Gly-14 and Arg-15 is the strongest of all the d_{NN} interactions. The strongest $d_{\alpha N}(i,i+2)$ interactions are between Pro-13 and Arg-15, and between Ala-16 and Val-18; however, the latter is accompanied by a much weaker d_{NN} interaction between Phe-17 and Val-18. These obsrvations indicate that the turn formed by the GPGR sequence is possibly more stable than the transient turns in other segments of the peptide. While the other segments of the two peptides exist partially in a helical conformation in TFE solutions, no medium-range interactions typical of a helical conformation were observed in the sequence GPGR.

Considering the chemical shifts of the amide protons, for most of them the average deviation in chemical shift (in absolute values) between P344 and RP135 is about 0.02 ppm in water and 0.04 ppm in 30% TFE/70% H_2O solution. Exceptionally, the amide protons of Gly-12, Gly-14, Arg-15, and Val-18 have deviations between 0.07 and 0.15 ppm. With regard to P547, the deviations in chemical shifts from the corresponding residues in RP135 are largest for the residues in the postulated turn GPGR. The similarity in chemical shift, together with the observation of similar CD spectra and similar interactions in the NOESY spectra, both in water and in H_2O/TFE solutions, indicates that the two short peptides fold like the corresponding parts in RP135, except that the transient turn in GPGR cannot be detected in the aqueous solution of P547. Therefore, we conclude that the N- and C-terminal parts of RP135 fold independently and there is no advantage in using the full-length RP135 as immunogen, to stabilize the conformation of its segments.

Chandrasekhar et al. (1991) studied the conformation of the PND peptide (RP142) of HIV-1_{MN}. The sequence comparison between RP135 and RP142 is given in Figure 1. RP135 shares only 56% sequence identity with RP142 and has two additional amino acids in one location and a deletion of one residue at another position in the sequence. On the basis of the observation of a strong NOE between the amide protons of Gly-14 and Arg-15 and a very weak NOE between the α-proton of Pro-13 and the amide proton of Arg-15, Chandrasekhar and his co-workers concluded that there is a significant population having a β-turn conformation in the sequence GPGR. It should be noted, however, that while a large number of NOE interactions between the amide protons of adjacent amino acids was observed, only one $d_{\alpha N}(i,i+2)$ interaction was detected. The latter interaction was not observed in a shorter version of RP142. Nascent helix conformations were not attributed to either of the HIV-1_{MN} peptides because of the absence of additional $d_{\alpha N}(i,i+2)$ interactions in their NOESY spectra measured in water. CD spectra of RP142 in TFE/water solutions measured by Chandrasekhar et al. (1991) and NMR data that were not presented were described as consistent with helix formation.

Larosa et al. (1990) predicted secondary structures of 245 PNDs by means of a neural network. They concluded that the most probable structure for the consensus sequence and for the IIIB isolate is β-strand–type II β-turn–β-strand–α-helix (the α-helix in the consensus peptide is beyond RP135). In their prediction, the β-turn is formed by the GPGR sequence. The notion of a turn in the GPGR sequence is supported by statistical analysis of the amino acid sequences of type I and type II turns (Wilmot et al., 1988). According to this analysis, type II turns favor proline at site $i+1$, glycine and asparagine at site $i+2$, and glutamine and arginine at site $i+3$; no specific preference was observed for the i position.

The predicted turn conformation of the GPGR sequence is further confirmed by Chandrasekhar et al. (1991) and by our NMR studies. However, unlike the prediction of Larosa et al. (1991), according to our finding the C-terminal segment of RP135 adopts nascent helix conformations, i.e., multiple turnlike conformations rapidly interconverting with an unfolded conformation. The N-terminal part of RP135 does not show any detectable tendency to form nascent helix conformations, although two interactions between adjacent amide protons were detected in this part of the peptide. It is possible that the mutations, deletions, and insertions in the amino acid sequences of the highly divergent PND peptides RP135 and RP142 modulate their tendency to form nascent helix conformations in water, without affecting the formation of a turn in the conserved GPGR sequence. The conformations of the PND in the native glycoprotein of the HIV-1 and when bound to HIV-1 neutralizing antibody, as well as mutational alterations of the determinant conformation in the protein, are some of the questions which should be addressed and which require further extensive studies.

SUPPLEMENTARY MATERIAL AVAILABLE

A table listing the chemical shifts assigned for peptides RP135 in 30% TFE, P344 in H_2O, P344 in 30% TFE, P547 in H_2O, and P547 in 30 and 60% TFE (6 pages) can be obtained upon request from the author.

REFERENCES

Bax, A., & Davis, D. G. (1985) *J. Magn. Reson. 65*, 355–360.
Bradley, E. K., Thomason, J. F., Cohen, F. E., Kosen, P. A., & Kuntz, I. D. (1990) *J. Mol. Biol. 215*, 607–622.
Chandrasekhar, K., Profy, A. T., & Dyson, H. J. (1991) *Biochemistry 30*, 9187–9194.
Chen, Y. H., Yang, T. J., & Chau, K. H. (1974) *Biochemistry 13*, 3350–3359.
Clore, G. M., Martin, S. R., & Gronenborn, A. M. (1986) *J. Mol. Biol. 191*, 553–561.
Dyson, H. J., Rance, M., Houghten, R. A., Wright, P. E., & Lerner, R. A. (1988) *J. Mol. Biol. 201*, 201–217.
Gorny, M. K., Xu, J., Gianakakos, V., Karwowska, S., Williams, C., Sheppard, H. Y., Hanson, C. V., & Zolla-Pazner, S. (1991) *Proc. Natl. Acad. Sci. U.S.A. 88*, 3238–3242.
Goudsmit, J., Debouck, C., Meloen, R. H., Smit, L., Bakker, M., Asher, D. M., Wolff, A. V., Gibbs, C. J., Jr., & Gajdusek, D. C. (1988) *Proc. Natl. Acad. Sci. U.S.A. 85*, 4478–4482.
Holley, L. H., Goudsmit, J., & Karplus, M. (1991) *Proc. Natl. Acad. Sci. U.S.A. 88*, 6800–6804.
Javaherian, K., Langlois, A. J., LaRosa, G. J., Profy, A. T., Bolognesi, D. P., Herlihy, W. C., Putney, S. D., & Matthews, T. J. (1990) *Science 250*, 1590–1593.
Larosa, G. J., Davide, J. P., Weinhold, K., Waterbury, J. A., Profy, A. T., Lewis, J. A., Langlois, A. J., Dreesman, G. R.,

Boswell, R. N., Shadduck, P., Holley, L. H., Karplus, M., Bolognesi, D. P., Matthews, T. J., Emini, E. A., & Putney, S. D. (1990) *Science 249*, 932–935.
Lehrman, S. R., Tuls, J. L., & Lund, M. (1990) *Biochemistry 29*, 5590–5596.
Liou, R., Rosen, E. M., Fung, M. S. C., Sun, W. N. C., Sun, C., Gordon, W., Chang, N. T., & Chang, T. W. (1989) *J. Immunol. 143*, 3967–3975.
Macura, S., Huang, Y., Suter, D., & Ernst, R. R. (1981) *J. Magn. Reson. 43*, 259–281.
Marion, D., & Wüthrich, K. (1983) *Biochem. Biophys. Res. Commun. 113*, 967–974.
Marion, D., Zasloff, M., & Bax, A. (1988) *FEBS Lett. 227*, 21–26.
Matsushita, S., Robert-Guroff, M., Rusche, J., Koito, A., Hattori, T., Hoshino, H., Javaherian, K., Takatsuki, K., & Putney, S. (1988) *J. Virol. 62*, 2107–2114.
Neuhaus, D., Wagner, G., Vasak, M., Kägi, J. H. R., & Wüthrich, K. (1985) *Eur. J. Biochem. 151*, 257–273.
Palker, T. J., Clarck, M. E., Langlois, A. J., Matthews, T. J., Weinhold, K. J., Randall, R. R., Bolognesi, D. P., & Haynes, B. F. (1988) *Proc. Natl. Acad. Sci. U.S.A. 85*, 1932–1936.
Palker, T. J., Matthews, T. J., Langlois, A., Kim, J. E., Berzofsky, J. A., Bolognesi, D. P., & Haynes, B. F. (1990) *UCLA Symp. Mol. Cell. Biol., New Ser. 119*, 313–322.
Plateau, P., & Guéron, M. (1982) *J. Am. Chem. Soc. 104*, 7310–7311.
Ratner, L., Haseltine, W., Patarca, R., Livak, K. J., Starcich, B., Josephs, S. F., Doran, E. R., Rafalski, J. A., Whitehorn, E. A., Baumeister, K., Ivanoff, L., Petteway, S. R., Jr., Pearson, M. L., Lautenberger, J. A., Papas, T. S., Ghrayeb, J., Chang, N. T., Gallo, R. C., & Wong-Staal, F. (1985) *Nature 313*, 277–284.
Robinson, W. E., Jr., Montefiori, D. C., Mitchell, W. M., Prince, A. M., Alter, H. J., Dreesman, G. R., & Elichberg, J. W. (1989) *Proc. Natl. Acad. Sci. U.S.A. 86*, 4710–4714.
Robinson, W. E., Jr., Kawamura, T., Gorny, M. K., Lake, D., Xu, J. Y., Matsumoto, Y., Sugano, T., Masuho, Y., Mitchell, W. W., Hersh, E., & Zola-Pazner, S. (1990) *Proc. Natl. Acad. Sci. U.S.A. 87*, 3185–3189.
Rusche, J. R., Javaherian, K., McDanal, C., Petro, J., Lynn, D. L., Grimaila, R., Langois, A., Gallo, R. C., Arthur, L. O., Fischinger, P. J., Bolognesi, D. P., Putney, S. D., & Matthews, T. J. (1988) *Proc. Natl. Acad. Sci. U.S.A. 85*, 3198–3202.
Scott, C. F., Jr., Silver, S., Profy, A. T., Putney, S. D., Langlois, A., Weinhold, K., & Robinson, J. E. (1990) *Proc. Natl. Acad. Sci. U.S.A. 87*, 8597–8601.
Skinner, M. A., Ting, R., Langlois, A. J., Weinhold, K. J., Lyerly, H. K., Jahaverian, K., & Matthews, T. J. (1988) *AIDS Res. Hum. Retroviruses 4*, 187–197.
Takahashi, H., Cohen, J., Hosmalin, A., Cease, K. B., Houghten, R., Cornette, J., De Lisi, C., Moss, B., Germain, R. N., & Berzofsky, J. A. (1988) *Proc. Natl. Acad. Sci. U.S.A. 85*, 3105–3109.
Takahashi, H., Germain, R. N., Moss, B., & Berzofsky, J. A. (1990) *J. Exp. Med. 171*, 571–576.
Takeda, A., Tuazon, C. U., & Ennis, F. A. (1988) *Science 242*, 580–583.
Wagner, G., Neuhaus, D., Wörgotter, E., Vasak, M., Kägi, J. H. R., & Wüthrich, K. (1986) *J. Mol. Biol. 187*, 131–135.
Wain-Hobson, S., Sonigo, P., Danos, O., Cole, S., & Alizon, M. (1985) *Cell 40*, 9.
Wang, C. Y., Looney, D. J., Li, M. L., Walfield, A. M., Ye, J., Hosein, B., Tam, J. P., & Wong-Staal, F. (1991) *Science 254*, 285–288.
Wilmot, C. M., & Thornton, J. M. (1988) *J. Mol. Biol. 203*, 221–232.
Wüthrich, K. (1986) *NMR of Proteins and Nucleic Acids*, Wiley, New York.
Wüthrich, K., Billeter, M., & Braun, W. (1984) *J. Mol. Biol. 180*, 715–740.